Journal of the Korean Nuclear Society
Volume 30, Number 6, pp.555~567, December 1998

Flare Test Evaluation and Stress Prediction of PWR' s Steam Generator Tubes

Woo-Gon Kim, Chang-Kyu Rhee, and Il-Hiun Kuk
Korea Atomic Energy Research Institute
150 Dukjin-dong, Yusong-gu, Taejon 305-353, Korea

Hae-Yong Cho and Sung-Chung Kim
Chungbuk National University
48 Gaeshin-dong, Heungduek-gu, Cheongju 361-763, Korea

(Received December 3, 1997)

Abstract

Alloy 600 and 690 steam generator tubes fabricated in Korea were evaluated by flare tests according to ASTM standards. The stress acting in the tube elements during the tests was predicted. All the tubes, including alloys 600 and 690, satisfied the requirement of a 30% or 35% O.D expansion. Flow curves obtained from the flare test were found to be higher in alloy 690 tubes than in alloy 600 ones. The difference between alloy 600 and 690 tubes increased gradually with flaring percentage (F.P,%). An effective stress corresponding to mean yield stress was introduced and calculated. It showed that the prediction values were in good agreement with the measured ones for all the 690 and 600 alloy tubes. It became possible to predict the amount of acting stresses within tubes during expansion process.

1. Introduction

Alloys 600 and 690 (UNS N06600 and N06690) have been widely used as the heat transfer tubing material of PWR' s steam generators. The tubes are required to keep superior stress corrosion cracking (SCC) resistance under corrosion environments, accompanying the service stresses of high temperature and pressure (310℃, 175 atm). If radioactive containing substances at the primary side leak to the secondary side owing to the degradation of the tubes, it may cause serious safety problems for nuclear power plants. Thus, it is important to evaluate the soundness of a manufactured tube[1-2]. For alloy 600, a lot of research work has been conducted to improve the corrosion resistance with partial success. A special heat treatment technique has been conducted for some time. Alloy 690, due to its superior corrosion resistance to alloy 600, has recently taken over alloy 600 in replaced or new steam generators[2-9].

In the assembly of steam generators, U-shaped tubes are fixed in the tubesheet with support from tube support plates (TSP) and the

ends of the tubes are expanded in the holes of the tubesheet by one of the such as explosive, mechanical and hydraulic methods[10]. The tensile residual stress induced by the expansion process is one of the important factors resulting in to the initial cracking, and the stress level changes with the method and degree of expansion, and along the position within tubes. Residual stresses existing after the expansion process can not be removed because the expansion process in the steam generator assembly is the last procedure which any thermal treatments do not follow[11-13]. Owing to the applied and residual stresses, any minor cracks can initiate failure under operating conditions of high temperature and pressure in nuclear power plant. Therefore, tube suppliers must show that the tube expansion procedure does not develop any minor cracks in the tubes[14]. It is also needed to predict accurately the acting stresses when a tube is assembled into the tubesheet hole.

In this study, the stress acting in the tube elements during the flare tests was predicted for alloy 600 and 690 tubes made in Korea. The theoretically-calculated stress for alloy 600 tubes, was well matched with the measured ones, but for alloy 690 tubes was not, as presented in a Kim' s previous study[15]. In order to predict an accurate stresses in tube expansion, an effective stress was introduced and calculated. It showed that the prediction results by effective stress were in good agreement with the measured ones for all the 690 and 600 alloy tubes. In this analysis, the used mechanical properties were obtained from the tensile test of the tube type. Microstructural changes after the flare test were also observed. This result can be utilized to predict stresses with the flaring percentage (F.P,%) when tubes are installed by the expansion process.

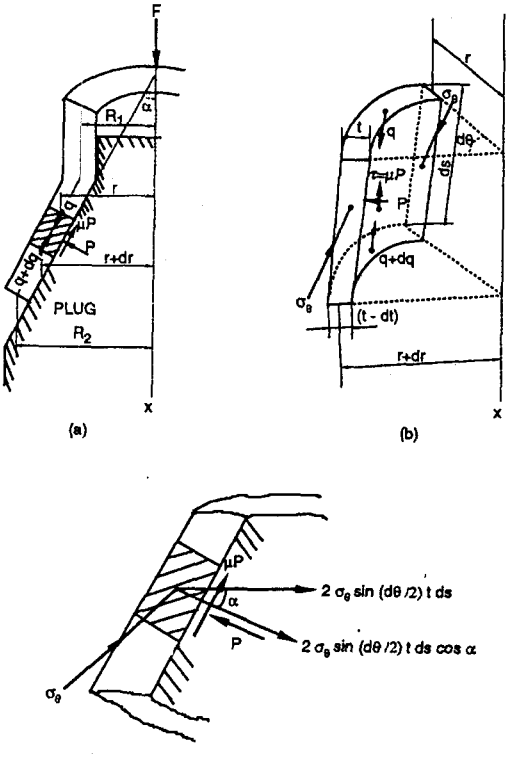

Fig. 1.(a) Schematic Diagram on the Tube Flaring with Conical Plug,α=30°
(b) Stresses Acting on the Small Fragmentary Element of the Tube
(c) Component of the Radial Force due to the Circumferential Stress, σ_θ, Exerted on an Element in a Direction Normal to the Plug Face

2. Theoretic Analysis

Fig. 1(a) shows the schematic tube section during a flare test with a conical plug of semisolid angle α. The tube with an initial diameter D_1 ($\approx 2R_1$) is flared by the conical plug until the diameter becomes D_2($=2R_2$). Each element within the tubes is under a quasi-static state during the flare test. Because outer diameter (O.D) of steam generator tube is

19.05 mm and the wall thickness is about 1.05 mm, we can therefore treat the tube thin[16] and can assume the variation in stress across the wall of the tube. Acting stresses at any mean radius of r are shown in Fig. 1(b), where q is the axial stress parallel to the plug face, σ_θ is hoop stress, p is the pressure perpendicular to the wall thickness, τ ($=\mu p$) is frictional stress between tube and plug, is the friction coefficient, t is the wall thickness at any mean radius of r, and ds is the length of an element parallel to the plug face.

The radial component of the force exerted on the element due to the hoop stress σ_θ, is 2 $\sigma_\theta \sin(d\theta/2)\ t$ ds, which has a component normal to the plug face, as shown in Fig. 1(c).

Considering the equilibrium between forces in the x and y directions and resolving forces exerted on the element in the directions normal and parallel to the plug face, and then simplifying, we can obtain the equilibrium differential equation for tube flaring, as reported in the previous study[15].

$$rt\left(\frac{dq}{dr}\right)+qt\left(\frac{dr}{dr}\right)-qr\left(\frac{dt}{dr}\right)+\sigma_\theta t+\mu\sigma_\theta t\cot\alpha=0. \quad (1)$$

Assuming the wall thickness constant during the process, $dt/dr \rightarrow 0$, equation (1) becomes

$$r\left(\frac{dq}{dr}\right)+q+\sigma_\theta(1+B)=0 \quad (2)$$

where $B = \mu \cot \alpha$. Since $t \cos(\alpha/r)$ is negligible in the case of a thin tube, the normal pressure to the plug, p, is smaller than the circumferential stress σ_θ. Hence, σ_θ(tensile) $\geq p \geq q$ (compressive) or $\sigma_1 = \sigma_\theta$, $\sigma_2 = p$ and $\sigma_3 = q$. If the normal pressure to the die, p, is negligible compared with the other two principal stresses, then the stress is considered as a plane stress, *i.e.*, $\sigma_2 = 0$. In the case of plane stress, there are two combinations of stresses to be considered. The von Mises criterion for yielding leads to $\sigma_1^2 - \sigma_1 + \sigma_3^2 = Y^2$, and the Tresca criterion for yielding leads to $\sigma_1 - \sigma_3 = Y$ [17]. The von Mises yield criterion is known to give the better prediction for yielding of most engineering metals. However, Tresca yield criterion gives a simpler mathematical approach when the magnitude and sign of principal stresses are known. Therefore, in this study we can use the modified Tresca yield criterion, *i.e.*,

$$\sigma_1 - \sigma_3 = mY \quad (3)$$

when m is a constant derived by the method of least squares and has an approximate value of 1.08. This value can be obtained from a graphical representation between the Tresca and von Mises yielding surfaces[17].

For a strain hardening material having a mean yield stress, $\overline{Y}$, the modified Tresca yield criterion gives

$$\sigma_\theta-(-q)=m\overline{Y} \quad (4)$$

or $$\sigma_\theta = m\overline{Y} - q. \quad (5)$$

Combining eqns. (2) and (5),

$$r\left(\frac{dq}{dr}\right)+Bq+m\overline{Y}(1+B)=0$$

$$\frac{dq}{[Bq-m\overline{Y}(1+B)]}=\frac{dr}{r}. \quad (6)$$

Integrating (6),

$$\left(\frac{1}{B}\right)\ln(Bq+C)=\ln r+\ln A,$$

$$C=-mY(1+B)$$

$$(Bq+C)^{1/B}=rA$$

where $\ln A$ is an integral constant.

Table 1. Chemical Compositions of Alloy 600 and 690 Tubes (wt%)

		Ni	Cr	C	Mn	Al	Fe	Co	S
ASTM requirements	UNSN 06600	72.0min.	14.0-17.0	0.15max.	1.0max.	-	6.0-10.0	0.5max.	0.015max.
	UNS N06690	58.0min.	27.0-31.0	0.05max.	0.5max.	-	7.0-11.0	0.5max.	0.015max.
K600		74.5	15.6	0.016	0.21	0.13	7.2	0.03	<0.001
K690		64.2	27.7	0.014	0.23	0.24	8.1	0.12	<0.001
I600		74.2	15.3	0.031	0.23	0.22	8.6	0.05	<0.001
I690		62.6	28.0	0.020	0.08	0.35	9.2	0.12	<0.001

I : INCO Tubes K : Tubes made in Korea

Because $q_1 = 0$ at the entrance to the plug (where $r = D_1/2$),

$$C^{1/B} = R_1 A \text{ or } A = C^{1/B}/R_1$$
$$(B_q + C)^{1/B} = (r/R_1) C^{1/B}$$
$$B_q + C = (r/R_1)^B C.$$

Therefore, the axial stress becomes

$$q = (C/B)[(r/R_1)^B - 1] \quad (7)$$

or $q = m\bar{Y}[(1+B)/B][1-(r/R_1)^B]$.

At the other end of the plug, where $r = D_2/2$, the axial stress, q_2, becomes

$$F \approx (\pi D_2 t/\cos\alpha) m\bar{Y}[(1+B)/B][1-(D_2/D_1)^B] \quad (8)$$

Hoop stress, σ_θ, can be obtained using equation (5) and the axial stress from equation (7). The axial force, F, is thus given by $F \approx q_2(\pi Dt/\cos\alpha)$. Therefore, the force variations can be computed with the F.P(%) as follows :

$$q_2 = m\bar{Y}[(1+B)/B][1-(D_2/D_1)^B]. \quad (9)$$

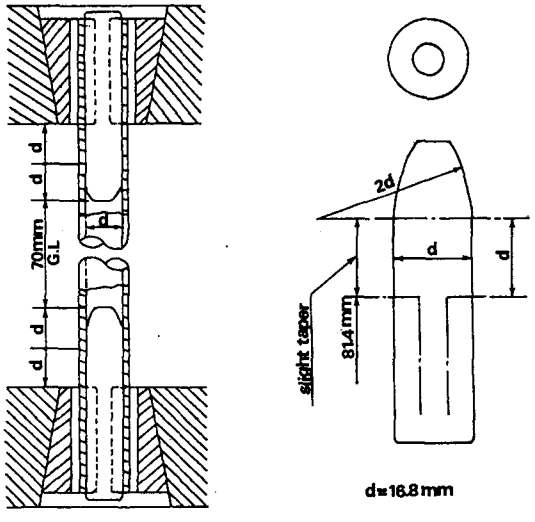

Fig. 2. Metal Plugs for Tensile Testing Alloy 600/690 Tubular Specimens

3. Experiment

Six different tubes were used in the flare test : K600-MA, K600-TT, I600-MA, K690-MA, K690-TT, and I690-MA. Series K was prepared by Sammi Special Steel Co. from alloy melting to mill annealing. Series I was manufactured using INCO' s forged bar. The MA series was

just a mill-annealed (1040℃/15min) one and TT series was heat treated (710℃/15hr) in a vacuum of 10^{-5} torr after mill annealing.

The chemical composition of the tubes is shown in Table 1. All the elements agree well with the composition range of the ASTM requirements (B167)[18], but the carbon contents in the K tubes reveal slightly lower amounts.

The tensile test specimens were 300mm in tube length and 70 mm in gauge length. Two steel plugs 100 mm long were inserted into both ends of the tube in order to support the tube from jaw pressure, as shown in Fig. 2. The tensile test was done with a 2.38×10^{-3}/sec strain rate at room temperature, following ASTM standards(E83)[19]. The yield strength in 0.2% off set value was measured.

Tube samples 50mm long were prepared for the flare test and both ends of the tubes were machined very slowly with lubricant to avoid any work hardening effect. According to ASTM standards on flare testing (B163)[14], an expanding tool was fabricated with an included angle of 60°. The material of the expanding tool was SKD-11 steel, the same material as used in the previous study[15]. Its surface was hardened by heat treatment. A schematic drawing of the expanding tool is shown in Fig. 3. Tubes were expanded by compression with expanding tools until the outside diameter of the tubes had increased by 30%. Expanded tubes were visually inspected after the flare tests.

The flare test was done using a universal tester with the strain rate of 1×10^{-3} /sec at room temperature. Lubricants between the expanding jig and the tube were not applied, i.e, the dry friction state. Microstructural changes were observed after the flare test, applying usual metallographic preparation and

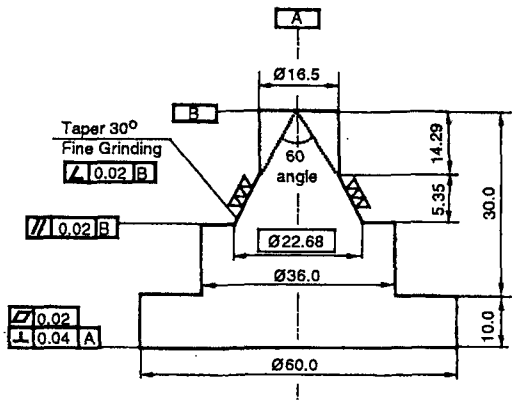

Fig. 3. Jig for Flare Test of Tubes

electrolytic etching (D.C 3 Volt/1 min) with 5 % nital solution.

4. Results and Discussion

4.1. Tube Evaluations and Flow Curves

Table 2 shows the results of the tensile test. The tensile and yield strengths of alloy 690 tubes are all higher than those of the alloy 600 ones, but the elongations are similar. After TT processing (thermal treatment at 710℃ for 15hr in a vacuum after mill annealing) the yield strength decrease by 8-16%, but the tensile strength was little changed although the major purpose of the thermal treatments is to improve the caustic SCC resistance by controlling the carbide distribution. In order to reduce the SCC threshold stress, it has been known that the yield strength is recommended to keep as low as possible[20]. The manufactured K as well as I tubes agree well with the ASTM requirements, as shown in Table 2.

Fig. 4 shows the applied force-flare percentage (F.P,%) flow curves. The flaring percentage (F.P,%) is presented as a function of the tube diameter as follows :

Table 2. Mechanical Properties of Alloy 600 and 690 Tubes

Specimens		Thermal Condition	YS(MPa) (0.2% Offset)	TS(MPa)	Elongation (%)
ASTM requirements	UNS N06600	Cold-worked annealed	240 min.	550	30min.
	UNS N06690	Cold-worked annealed	240 min.	586	30 min.
MA	K600-MA	1040℃/15min	407	698	34
	I600-MA	1040℃/15min	382	735	36
	K690-MA	1040℃/15min	412	792	38
	I690-MA	1040℃/15min	450	785	37
TT	K600-TT	MA+710℃/15hr	340	696	36
	K690-TT	MA+710℃/15hr	380	791	38

* MA : Mill Annealed TT : Thermally Treated
I : INCO Tubes K : Tubes made in Korea

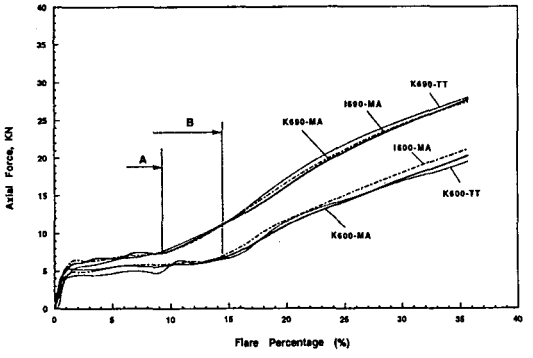

Fig. 4. Flow Curves of Force-F.P(%) Plotted by the Flare Test in Various Alloy 600 and 690 Tubes

$$F.P\ (\%) = (D_f - D_o) / D_o \times 100 \qquad (10)$$

where D_o is the initial diameter and D_f is the flared diameter. As the flare percentage increases, the applied force increases. More force was needed for the alloy 690 tube than for the alloy 600 tube at the same flare percentage(%). There were some difference between the alloy 600 and 690 tubes at the transient region of an initial flaring stage. That is, in the alloy 600 tubes the axial force (B region in Fig. 4) was little changed up to 15% flare percentage, and in the alloy 690 tubes to 10% flare percentage (A region in Fig. 4). It was considered that the higher work hardening effect in the alloy 690 could attribute to the higher Cr content, respectively. The tensile strength and elongation of the alloy 690 tubes were similar to those of the alloy 600, respectively, but the yield strength was much higher than that of the alloy 600(Table 2). Thus, the tendency of flow curves depend on the material strengths : alloy 600 or 690, and thermal treatment conditions(MA or TT).

Fig. 5 shows the microstructures before the flare test of alloy 600 and 690 MA tubes. In the case of alloy 690 tubes (c,d) many twin faces

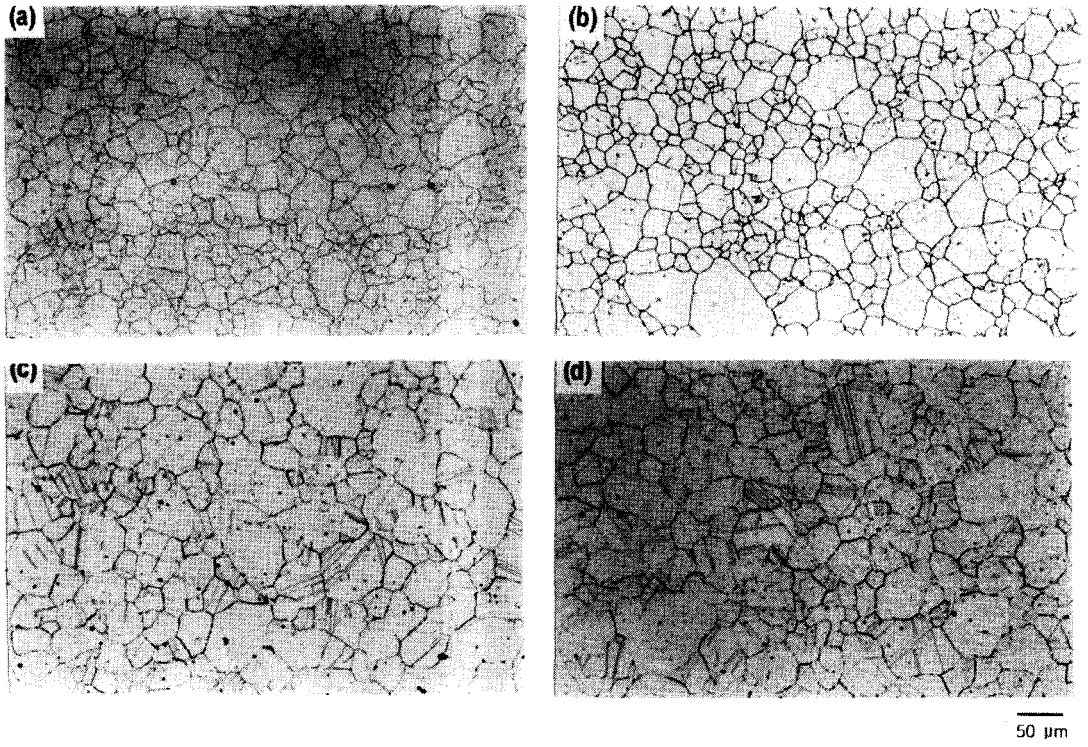

Fig. 5. Optical Microstructures Before the Flare Test of Mill Annealed Tubes:(a) K600-MA, (b) 1600-MA, (c) K690-MA, (d) 1690-MA

were observed in the grains, and carbide precipitates were distributed along the grain boundaries. Distributions of the precipitates resulting from thermal treatment conditions may affect the SCC resistance of materials. The microstructures of INCO and domestic K-tubes were similar.

Fig. 6 shows the microstructures of alloy 600 tubes after a 35% O.D expansion flare test. Figs. 6 (a) and (c) show the plane view of flared O.D surface, where, the horizontal direction is hoop deformation, and Figs. (b) and (d) show the perpendicular cross section of an O.D surface, where the vertical direction is a hoop deformation. Fig.6 shows clearly that grains are elongated by hoop stress. Therefore, hoop stress, σ_θ was more dominant than the axial stress, q.

After O.D expansion, the tubes were checked visually along the flared wall to see whether any minor cracks existed or not. No minor crack was found with a 30%, or even 35%, O.D expansion for all tubes. Thus, all the tubes were evaluated to be good with regards to flaring behavior. Fig. 7 shows the plane view of a 30% O.D flared tube.

4.2. Stress Calculation

Stress analysis on tubes was performed assuming for a rigid perfectly-plastic body. Acting stresses such as σ_θ, q, and F during the flare test were calculated using eqns (4), (7), and (8). The friction coefficient , and constant m,

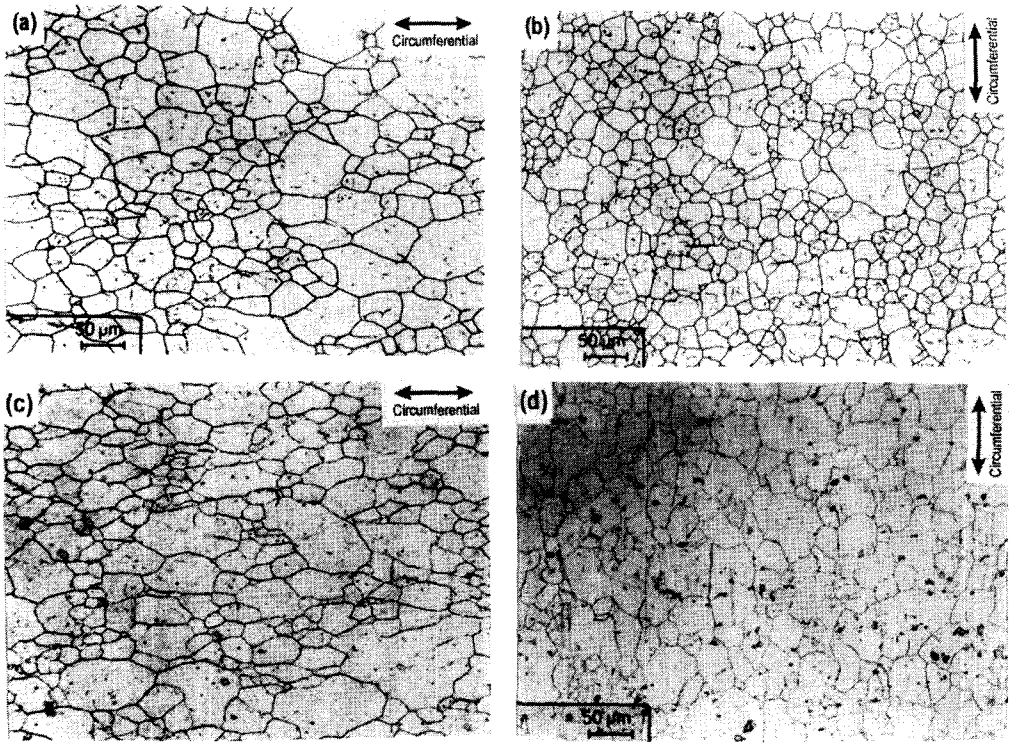

Fig. 6. Optical Microstructures Showing Circumferential and Axial Direction Deformation after Flare Tested Tubes(a,b : K600-MA, c,d : K690-TT)

were assumed as 0.2 and 1.08, respectively. The semisolid angle of the plug, α, was 30°. The wall thickness change during the test was neglected. In the previous study[15], a theoretically-calculated stress for alloy 690 tubes was not consistency with the measured one[15]. The strain hardening effects of materials were not considered in the plastic region. Namely, the 0.2% offset value of the yield strength was used. The calculated stresses were therefore lower than those of the measured ones.

This study suggests that the strain hardening effects be considered, because Nickel base alloy has the strain hardening effects as solid-solution hardened materials[21]. It is therefore possible to introduce the effective stress, which is the

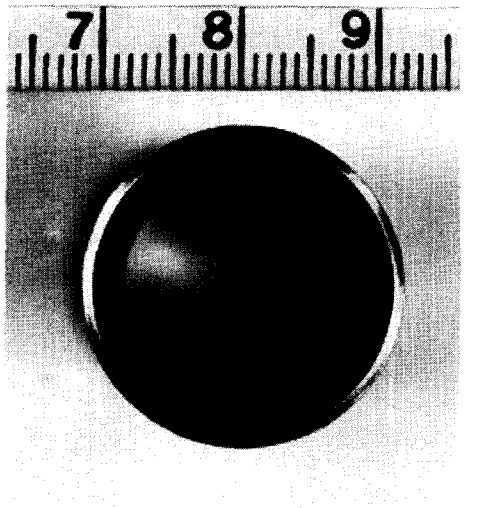

Fig. 7. Plane View of 30% O.D Flared Tube

Table 3. Mean Yield Stress for Various Tubes

Materials / Effective Stress	K600-MA	I600-MA	K690-MA	I690-MA	K600-TT	K690-TT
$\overline{Y}$	491	528	570	586	483	578

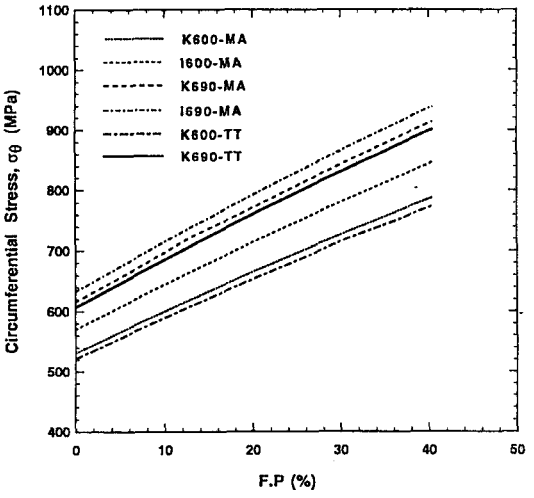

Fig. 8. Circumferential Stress(σ_θ) Analysis with F.P(%) on Various Tubes

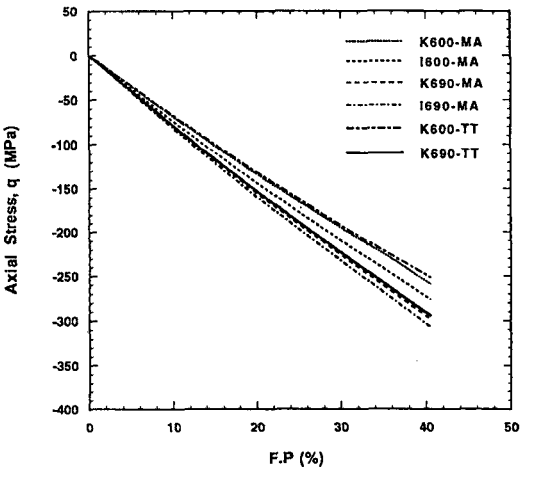

Fig. 9. Axial Stress(q) Analysis with F.P(%) on Various Tubes

new yield strength due to the effect of cold working. In order to quantify reasonably the mean yield strength as a function of cold working, the loading is taken to be 1(uniaxial stress), and isotropy and volume constancy are assumed. It can be written that [22]

$$\sigma_1 = \bar{\sigma} \text{ and } d\varepsilon_1 = d\bar{\varepsilon}. \tag{11}$$

Thus, the tensile results are, in fact, descriptive of an effective stress-strain plot. For this reason it can be written as follows :

$$\bar{\sigma} = \sigma_0 + K\bar{\varepsilon}^n = Y \tag{12}$$

where σ_0 is stress to elastic region, and K and n are material constant. This equation may be more satisfied than that of $K\bar{\varepsilon}^n$. From this point on, we can use an effective stress. The mean yield stress corresponding to the effective stress was obtained graphically by using the tensile plot. Determination of the effective stress was obtained by taking an areal average, which is the mean of the total energy stored to tensile strength(UTS) from zero stress.

Mean yield stresses($\overline{Y}$) obtained from all the tubes are presented in Table 3. It appears that $\overline{Y}$ values are higher than 0.2% offset yield strengths due to the strain-hardening effects, while $\overline{Y}$ values are lower than flow stresses that are the averages of yield and tensile strength.

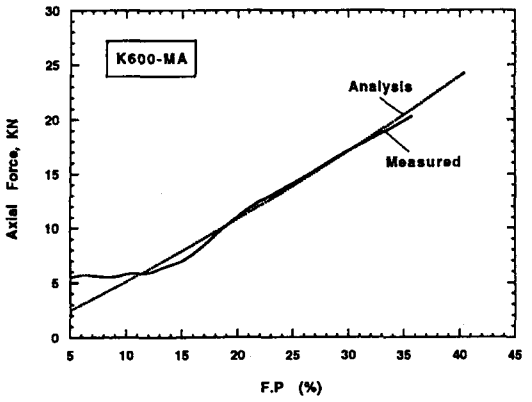

Fig. 10. Comparision of Analytical and Measured Flow Curves with F.P(%) in K600-MA Tube

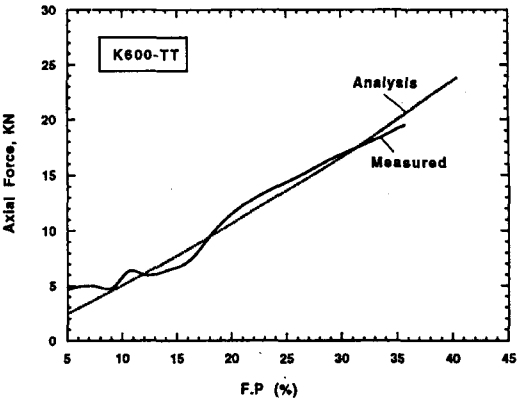

Fig. 11. Comparision of Analytical and Measured Flow Curves with F.P(%) in K600-TT Tube

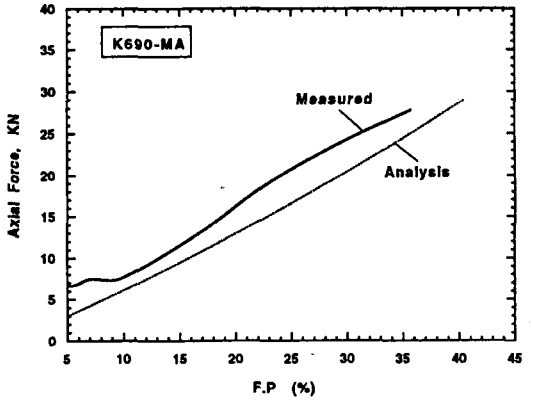

Fig. 12. Comparision of Analytical and Measured Flow Curves with F.P(%) in K690-MA Tube

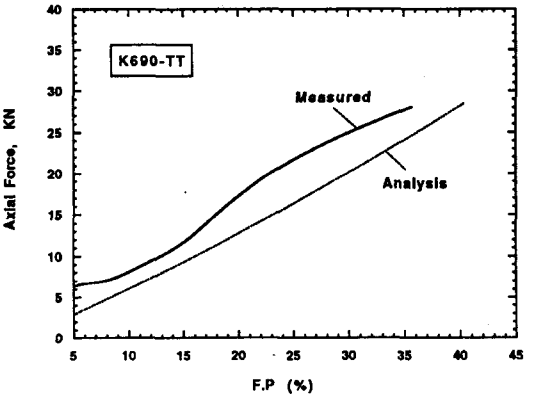

Fig. 13. Comparision of Analytical and Measured Flow Curves with F.P(%) in K690-TT Tube

The calculated values of σ_θ and q in the alloy 600 tubes are shown Figs 8 and 9, respectively. Hoop stress, σ_θ, increases almost linearly with flare percentage (%). However the axial stress, q, shows a negative(-) value, *i.e.*, compressive stress, with some deviations among the tubes (Fig. 9). The slope is the highest in the I690-MA tube and the lowest in the K600-TT.

Figs. 10 and 11 illustrate the calculated and measured curves of the axial compressive force, F, during the tests of the alloy 600 tubes. The calculated values for the K600-MA and K600-TT tubes are very close to the measured ones after the transition region of about 10% expansion.

Figs. 12 and 13 illustrate the calculated and measured curves of the axial compressive force, F, during the tests of alloy 690 tubes. The

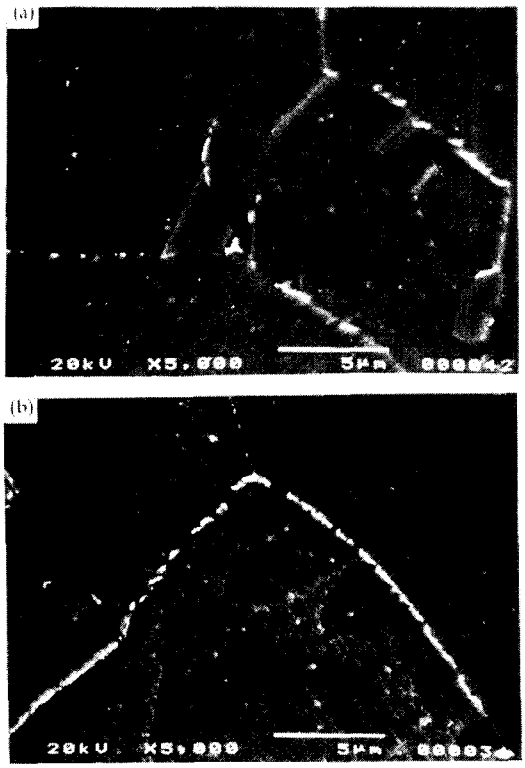

Fig. 14. Scanning Electron Micrographs of (a) K690-MA and (b) K690-TT Tubes (Etchant ; Bromine-Methanol Solution)

calculated values are almost close to the measured ones.

The gaps in the flow curves of TT tubes, rather than MA ones, seem to be mainly attributed to decrease in yield strength due to the stress relief effect following more precipitates of chromium carbide along the grain boundaries, as shown in Figure 14(a,b). Although the main goal of TT treatment is not stress relieving, the carbide precipitate density becomes higher. Therefore, it seems to influence the mechanical properties (including flaring behavior) due to a further decrease of dislocation and the supersaturated solid solution hardening element(e.g chromium) than the carbide morphology itself.

In addition, the gaps of the alloy 690 tubes with F.P(%) increases seems to be attributed to the higher Cr contents, which may cause more work hardening effects due to the twin boundary, as shown in Fig. 5 (c,d).

Consequently, it became possible to predict the amount of acting stresses within tubes during expansion processes using derived equations. The flow curves for various tubes depend on the mechanical properties due to the material parameters and thermal treatment conditions: alloy 600 or 690, and MA or TT.

5. Conclusions

Alloy 600 and 690 tubes made in Korea met with the ASTM flare test requirements. No minor cracks were found until a 30% and 35% O.D expansion. The flow curves measured during the flare tests were steeper in 690 than 600 tubes and the gap increased gradually with the flaring percentage(F.P,%). Calculated stresses in the flare test agreed well with the measured ones for all tubes, but deviated slightly from the measured ones for alloy 690 tubes. This behavior seems to be attributed to the large chromium content in alloy 690 and the bigger solid solution hardening effect. The tendency of the flow curves for various tubes depends on the material parameters and thermal treatment conditions : alloy 600 or 690, and MA or TT. From this result, it was possible to predict the amount of acting forces or stresses with F.P(%) when the tubes were installed into the tubesheet by expansion process.

References

1. H. Widmark, "Materials for the Nuclear Power Industry", *Sandvik Steel*, November (1986).

2. Cebelcor, "Steam Generator Corrosion Studies", EPRI NP-2331, April (1982).
3. G.J. Theus, "Stress Corrosion Cracking of 600 and Alloy 690 in All Volite Treated Water at Elevated Temperatures", *EPRI NP-3061*, May (1983).
4. J.F. Newman, "Stress Corrosion of Alloy 600 and 690 in Acidic Sulfate Solutions at Elevated Temperatures", *EPRI NP-3043*, October (1983).
5. A.Smith,et al., "Relationship between Composition, Microstructure and Corrosion Behavior of Alloy 690 Steam Generator Tubing for PWR Systems" , *Fourth International Symposium on Environmental Degradation of Materials in Nuclear Power Systems-Water Reactors*, pp 33-46 August (1989).
6. D.L. Harrod, et al., "The Temperature Depedenance of Tensile Properties of Thermally Treated Alloy 690 Tubing", *Fifth International Symposium on Environmental Degradation of Materials in Nuclear Power Systems-Water Reactors*, pp 849-854, August 25-29 (1991).
7. F. Cattant, et al., "Effectiveness of 700oC Thermally Treatment on Primary Water Stress Corrosion Sensitivity of 600 Steam Generator Tubes", *Fifth International Symposium on Environmental Degradation of Materials in Nuclear Power Systems-Water Reactors*, pp 901-913, August 25-29 (1991).
8. G.P. Airey, "Optimization of Metallurgical Variables to Improve the Stress Corrosion Resistance of Inconel 600", *EPRI NP-1354*, March (1980).
9. W.C. Kim, et al., "Studies Related to the Secondary-Side SCC Evaluations in Steam Generator Tubes of Nuclear Power Plants", *KAERI/RR-765/88*, pp 84-87, December (1988).
10. W.S. Rhu, " Study on Thermal & Mechanical Properties of U-Tube Material for Steam Generator, *KAERI/RR-1990/92*, December (1992).
11. R. McGregor, et al., "Experimental Residual Stress Evaluation of Hydraulic Expansion Transitions in Alloy 690 Steam Generator Tubing", Seventh International Symposium on Environmental Degradation of Materials in Nuclear Power Systems-Water Reactors, Vol.1, pp 495-507, August 7-10 (1995).
12. J. Woodward, et al., "Stress Relief to Prevent Stress Corrosion in the Transition Region of Expanded Alloy 600 Steam Generator Tubing", *EPRI NP-3055*, May (1983).
13. G.V. Amoruso, et al., "Stress Corrosion Cracking Test of Expanded Steam Generator Tubes", *EPRI-NP5012*, January (1987).
14. ASTM, " Standard Specification for Seamless Nickel and Nickel Alloy Condenser and Heat Exchanger Tubes", *ASTM Designation B163-86a*, pp 62-63, March (1986).
15. W.G. Kim, J. Jang and I.H. Kuk, "Flare Test and Stress Analysis of Alloy 600/690 Tubes", *Journal of the Korean Nuclear Society*, Vol.29, No.2, pp 138-147, April (1997).
16. M.F. Spotts, "Mechanical Design Analysis", *Engle Cliffs, New Jersey*, pp 122-123, (1964)
17. A.C. Ugral, et al., "Advanced Strength and Applied Elasticity", 3rd Edition, *Prentice Hall PTR, New Jersey*, pp154-157, (1995).
18. ASTM, "Standard Specifications for Nickel-Chromium-Iron Alloys (UNS N06600 and N06690) Seamless Pipe abd Tube", *ASTM*

Designation B167-86, pp 92-98, April (1986).

19. ASTM, "Standard Test Methods of Tension Testing of Metallic Materials", *ASTM Designation E8-87a*, pp 121-134, May (1988).
20. I.H. Kuk, et al., "Advanced Nuclear Material Development/Steam Generator Material", *KAERI/RR-1764/96*, Final Report, p215, September (1997).
21. S.Y. Hong, et al., "Characterization of Mechanical Properties of Inconel Alloys", *KAERI/ CM-081/94,* August (1995).
22. W. F. Hosford and R.M. Caddell, "Metal Forming : Mechanics and Metallurgy", Prentice Hall, Inc., Englewood Cliffs, N.J. 07632, pp 49-55 (1983).